GEM TN-92-161

Generation of a Precisely Timed Muon Trigger Using Signals from the GEM Drift Tubes

L. Barabash, C. Bromberg, Yu. Fisyak, N. Lau, D. Marlow, R. Miller, G. Mitselmakher, A. Wang, and V. Zhukov

August 24, 1992

Abstract:

An approach for generation of a muon trigger signal with a time resolution good enough to identify the bunch crossing is described. The proposed circuit provides a timing pulse that is independent of the position and angle of incidence. The pulse is delayed with respect to the muon time of arrival by a constant amount, approximately equal to the total drift time in a single cell.

Generation of a Precisely Timed Muon Trigger Using Signals from the GEM Drift Tubes

L.Barabash, C.Bromberg, Yu.Fisyak, N.Lau, D.Marlow,
R.Miller, G.Mitselmakher, A. Wang, V.Zhukov

August 24, 1992

Abstract

An approach for generation of a muon trigger signal with a time resolution good enough to identify the bunch crossing is described. The proposed circuit provides a timing pulse that is independent of the position and angle of incidence. The pulse is delayed with respect to the muon time of arrival by a constant amount, approximately equal to the total drift time in a single cell.

1 Algorithm for Absolute Time-of-Flight Measurements

The absolute time of arrival of particles passing through drift detectors can be calculated using the information from three drift gaps. In particular, for the three-layer geometry shown in figure 1, we have

$$T_{\text{tot}} = \frac{(T_1 + T_3)}{2} + T_2 \tag{1}$$

where T_1, T_2, and T_3 are the arrival times of the pulses generated at the anode wires, W_1, W_2, and W_3, respectively. Taking into account the resulting symmetry about $T_{\text{tot}}/2$ one can calculate the absolute time of arrival of the particle, provided that the drift velocity and total drift time T_{tot} are known. To be specific, we calculate the value of x, which is the length of the time interval between the arrival of the latest pulse and the total drift time in terms of t_1 and t_2, defined by

$$t_1 = |T_2 - \max(T_1, T_3)| \quad \text{and} \quad t_2 = |T_1 - T_3| \tag{2}$$

as shown in figure 1.

Figure 2 shows different time situations generated by a particle passing through the chamber. The three pictures describe situations where a muon track doesn't cross the boundary of three half-cells—i.e. the "simple case". In this instance, x can be found from the relation

$$\text{Solution 1}: \qquad x = \frac{T_{\text{tot}}}{2} - \left(\frac{t_1}{2} + \frac{t_2}{4}\right) \tag{3}$$

More complex situations arise when the muon track passes through the boundary of a cell. For these events we obtain three additional relations covering different angular ranges.

$$\text{Solution 2}: \qquad x = \frac{t_2}{2} - t_1 \tag{4}$$

$$\text{Solution 3}: \qquad x = T_{\text{tot}} - \left(t_1 + \frac{t_2}{2}\right) \tag{5}$$

$$\text{Solution 4}: \qquad x = \frac{t_2}{2} \tag{6}$$

In each case the trigger works by generating a pulse at a time determined by the arrival of the last pulse and the interval x. As noted, this pulse will occur a fixed time after the particle traverses the chamber array.

Figure 3 shows the areas in which the various solutions apply in terms of the position and angle of incidence. Calculations were made for 20-mm-radius drift tubes arranged in a hex-packed array (see figure 3a), as will be the case for the GEM PDT's. One of the sensitive wires of the first layer of a triplet is taken as coordinate system origin. As seen from figure 3b, these solutions cover an angular range up to 16° and have different configurations in this coverage. From figure 3b one sees that for $|\phi| < 16°$, solution 1 applies 50% of the time while either solution 2,3, or 4 applies to the remaining cases.

In the simplest implementation each of the four solutions generates a pulse, leading to the possibility of false triggers. In what follows we show how nearly all false triggers can be rejected by combining the results from a pair of triplets, A and B, arranged as shown in figure 5c.

The right-hand plots in figure 4a show the distribution of pulse times from all four solutions for triplets A and B. The 2736 entries in the these plots are the result of 684 tracks generated in 1 mm steps in incident position over the range 0mm $< X <$ 40 mm (excluding $X = 0, 20,$ and, 40 mm) and in one degree steps in ϕ over the range $0 < \phi <$ 17°. The peak at $t = 0$ corresponds to the correct solution, while the flat out-of-time background is the result of ghost pulses from the "wrong" solutions. Since early trigger pulses would effectively blind the trigger system to the correct solution, the large ($\sim$ 50%) fraction of events with early pulses from either of the triplets alone would not provide acceptable operation.

However, the following conditions can be used to reject false triggers:

- Triggers from solution 3 can be separated from the other solutions if the layers are connected as shown in figure 5.b.
- A significant portion of false triggers from solution 2 can be rejected because they result in negative values of $x \leq 0$.
- In the simple case where the track crosses no half-cell boundaries, it is generally true that solutions 4 and/or solutions 2 from triplets A and B are equal. In these cases, solution 1 can be selected.

The time spectra from the A & B triplets after the application of these criteria are shown in the right-hand plots of figure 4a. The number of false early triggers has been significantly reduced.

Finally, complete rejection of false triggers is achieved over the angular range of interest by requiring a coincidence between the outputs of triplets A and B. The resulting time spectrum is shown in figure 4b.

For stiff tracks in GEM, the maximum angle of incidence, which is 11°, is determined by the 16-fold azimuthal segmentation of the GEM muon array. Thus the method just described is efficient for muon bending angles as large as 5° (total ϕ angle of 16°), corresponding to momenta of 10 GeV/c or more. The use of 32-fold azimuthal segmentation would reduce the number of equations, since solution 2 could be excluded (see figure 3b).

2 Implementation

Figure 6 shows a possible electronic realization of the proposed scheme. The circuit employs binary counters and digital summing registers to implement Solution 1. The other solutions can be done in similar ways. Additional circuitry can be used to make corrections for non-linearity in the time-distance relation and other such effects. The details of the implementation are not discussed here, but will be the focus of future efforts.

3 Estimation of the Efficiency

The equations above apply for a single incident particle. In cases where extra hits occur due to the production of δ-rays in the gas, bremsstrahlung of high energy muons in the calorimeter or muon detector walls, punchthrough, accidental hits from neutrons, or detector noise, a loss of efficiency may result. Each of these effects must be estimated carefully and will be the subject of future studies.

For now we note that the magnetic field serves to partially mitigate the effect of δ-rays, as shown figure 7. In addition we estimate the tolerable counting rates from random sources below.

One can estimate the admissible level of accidental (e.g. neutron) hits as follows. The accidental triple coincidence rate in a single superlayer, R_3, is approximately given by

$$R_3 = \tau^2 R_1^3 \tag{7}$$

where R_1 is the singles rate for one wire and τ is the effective resolving time of the coincidence. Taking $\tau = 1$ μs, one concludes that the rate per layer must be limited to less than a few time 10^4 Hz. Although the effects of accidentals can be further mitigated by placing two or more superlayers in coincidence, high singles rates also lead to a loss of efficiency due to circuit deadtime. Since the time scale for this is also 1μs, one is once again led to conclude that the singles rates should be limited to the few times 10^4 level. This will determine the number of tubes that can be safely ganged together.

4 Future Plans

This algorithm can be checked during the test of muon detectors. As a first step it can be evaluated without additional electronics by using the measured leading edge times T_1, T_2, and T_3 as input to an offline analysis. Direct measurement of the time intervals t_1, t_2 and x is even more interesting and could be achieved with relatively simple circuitry (e.g. in NIM logic). These tests will serve to establish the general viability of the technique.

5 Acknowledgements

We would like to acknowledge useful discussions with M. Marx, M. Atiya, and F. Stocker.

6 Figure Captions

Fig.1. Principle of muon trigger generation.

Fig.2. Different situations arising in drift tubes ("simple case")

Fig.3.a. and 3.b. Angle and coordinate ranges covered the by the different solutions.

Fig.4.a. Time distributions of decisions from solutions 1,2,3 and 4 before in triplets A and B.

Fig.4.b. Time distribution of triggers after coincidence between two triplets in superlayer of the drift tubes.

Fig.5. a — simple connection of the drift tubes in triplet,
b — connection for separation solution 3.
c — connection of the drift tubes in superlayer.

Fig.6. Block diagram of one possible electronic realization.

Fig.7. Muon track and δ - ray tracks in a drift tube.

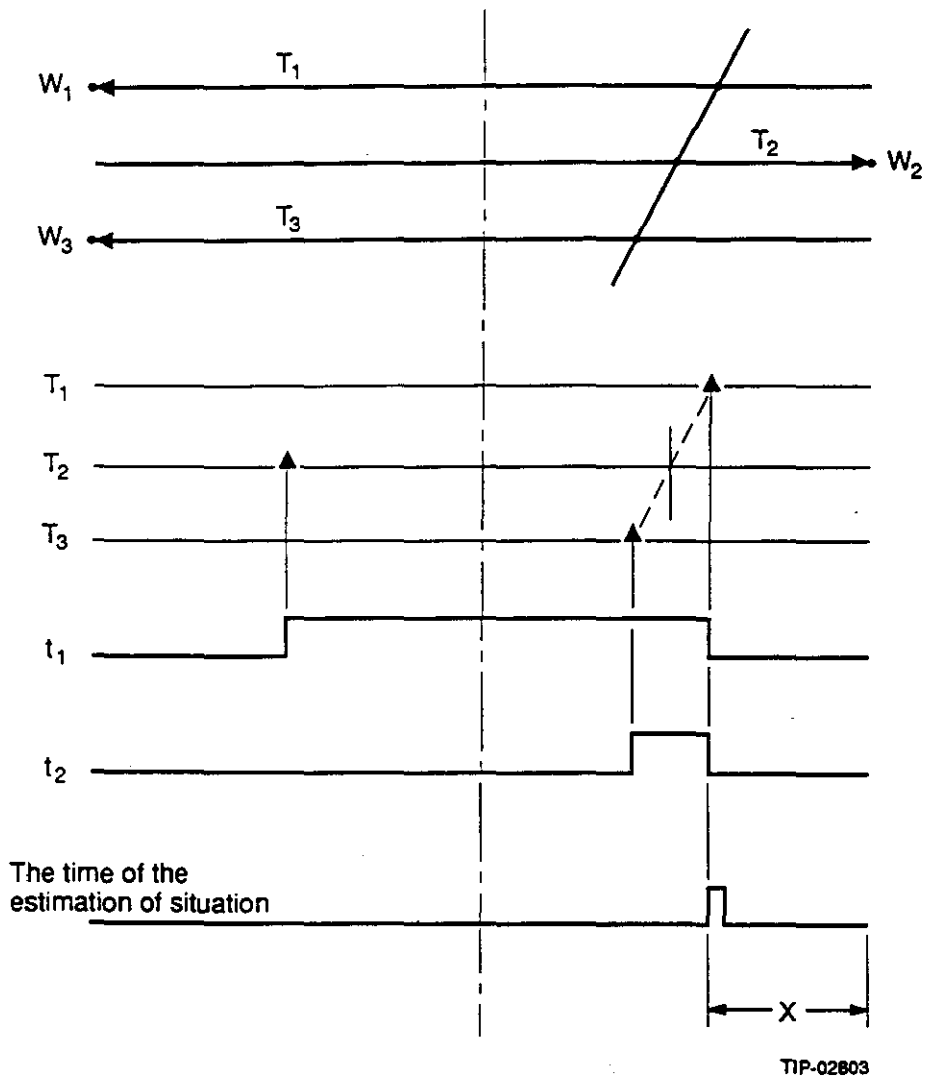
W1
T1
T2
W2
W3
T3
T1
T2
T3
t1
t2
The time of the
estimation of situation
X
TIP-02803

Fig.1.

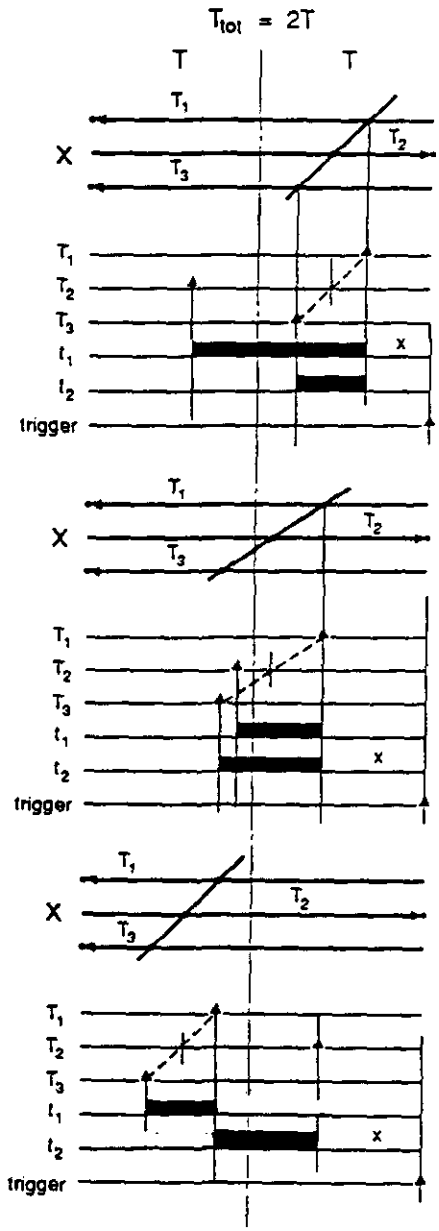

$$x = T - \left(\frac{t_1}{2} + \frac{t_2}{4} \right)$$

$$x = T - \left(\frac{t_1}{2} + \frac{t_2}{4} \right)$$

$$x = T - \left(\frac{t_1}{2} + \frac{t_2}{4} \right)$$

TIP-02804

Fig.2.

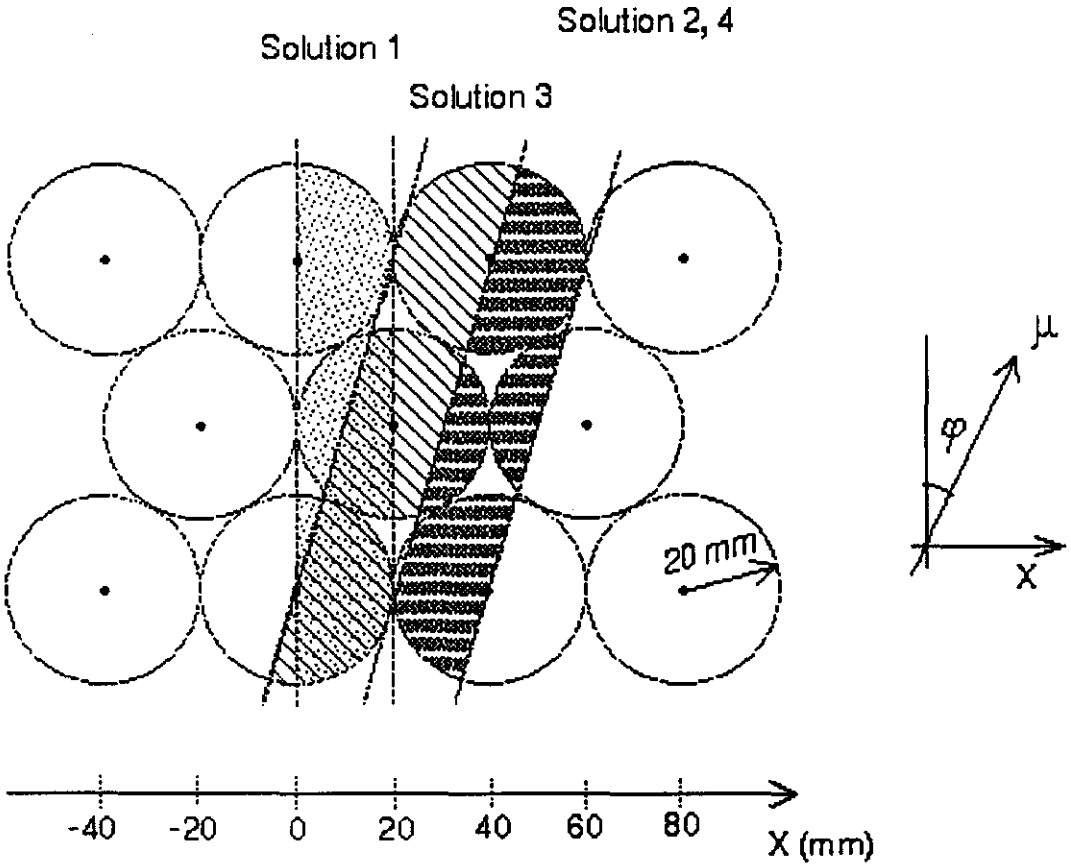
Solution 1
Solution 2, 4
Solution 3
20 mm
-40
-20
0
20
40
60
80
X (mm)
μ
φ
X

Figure 3a

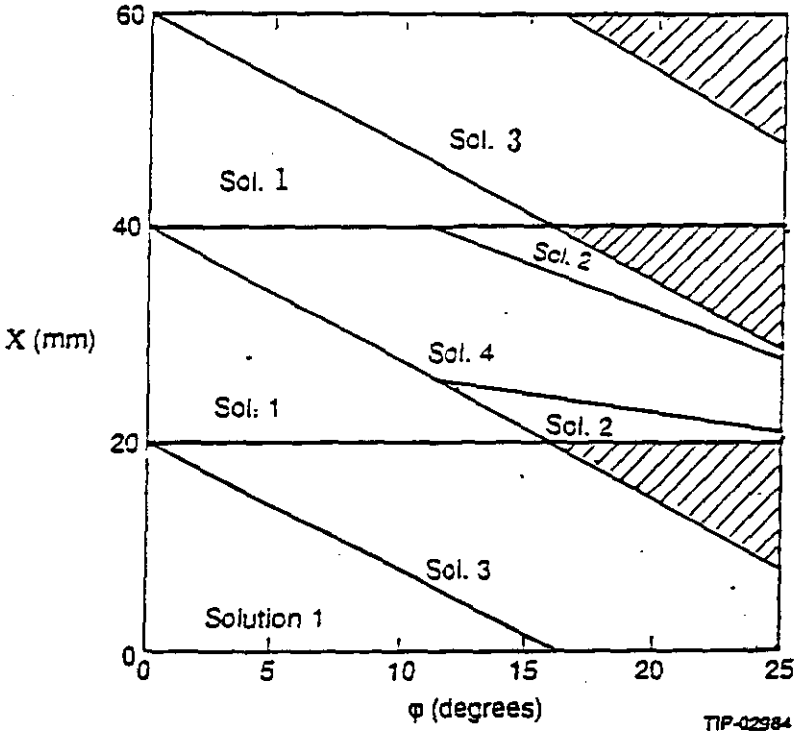
60
40
20
0
X (mm)
Sol. 3
Sol. 1
Sol. 2
Sol. 4
Sol. 1
Sol. 2
Sol. 3
Solution 1
0
5
10
15
20
25
φ (degrees)
TIP-02984

Fig.3.b.

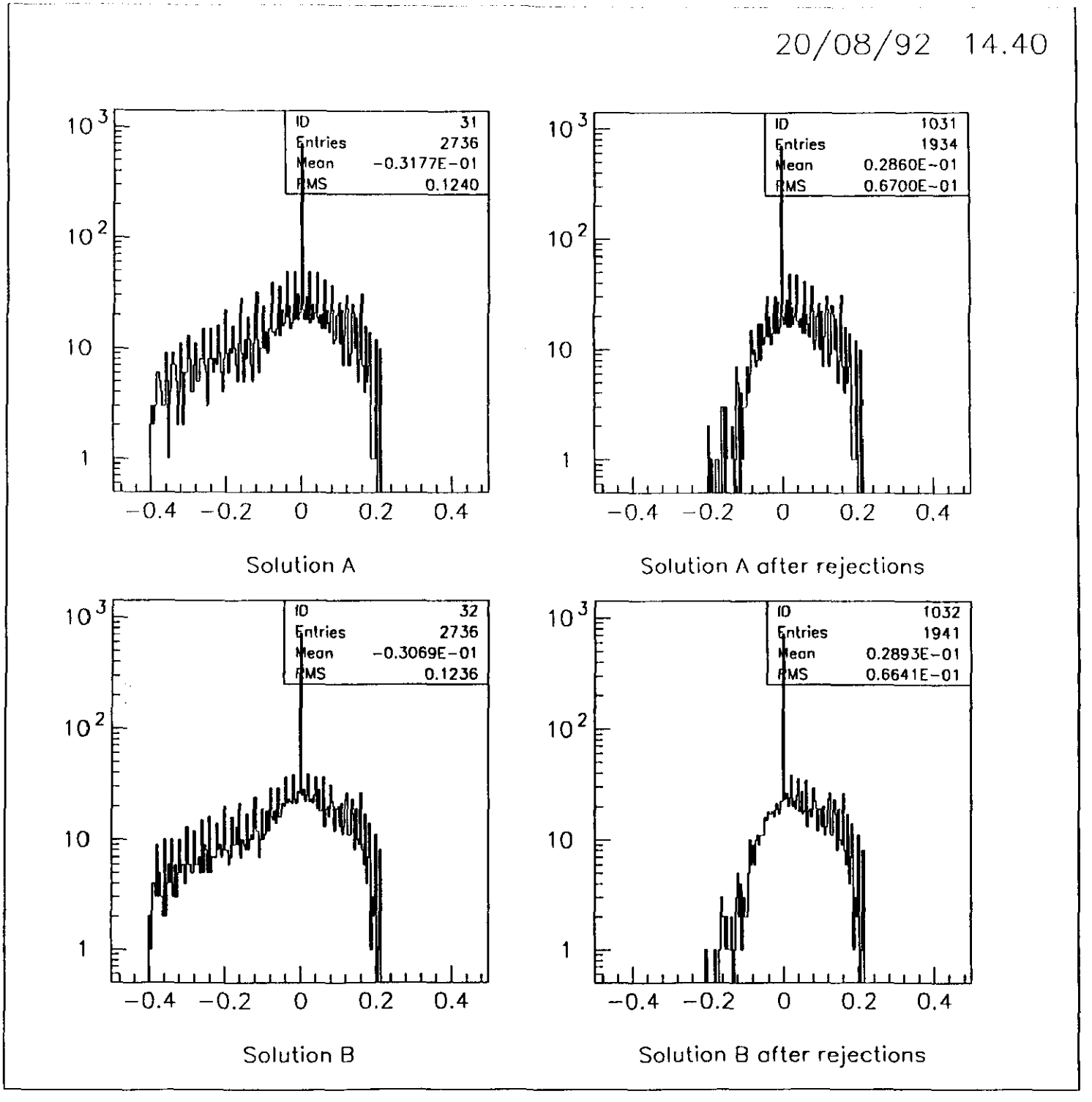
20/08/92 14.40
ID 31
Entries 2736
Mean -0.3177E-01
RMS 0.1240
Solution A
ID 1031
Entries 1934
Mean 0.2860E-01
RMS 0.6700E-01
Solution A after rejections
ID 32
Entries 2736
Mean -0.3069E-01
RMS 0.1236
Solution B
ID 1032
Entries 1941
Mean 0.2893E-01
RMS 0.6641E-01
Solution B after rejections

Fig.4.a.

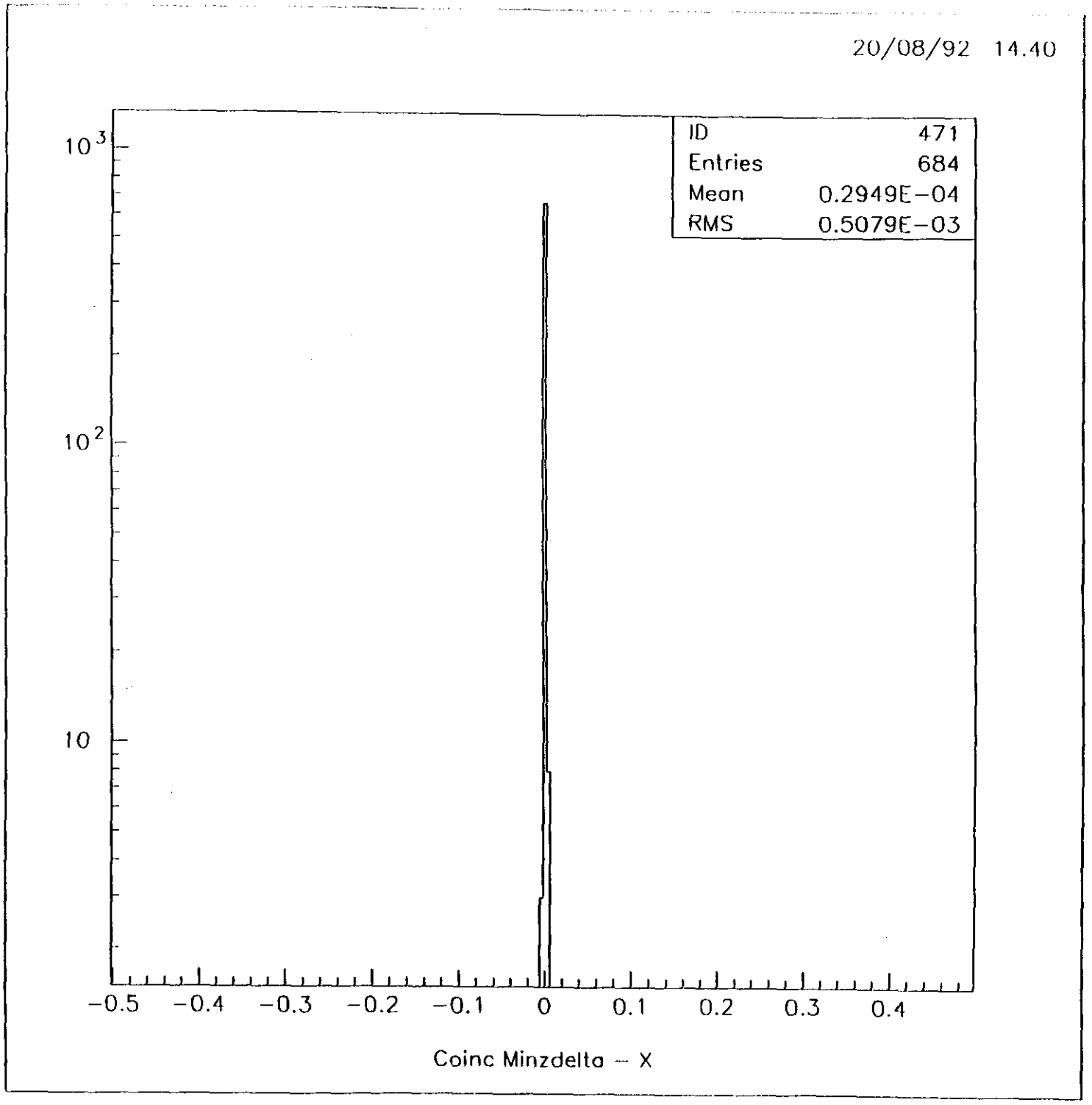
20/08/92 14.40
ID 471
Entries 684
Mean 0.2949E−04
RMS 0.5079E−03
10³
10²
10
−0.5
−0.4
−0.3
−0.2
−0.1
0
0.1
0.2
0.3
0.4
Coinc Minzdelta − X

Fig.4.b.

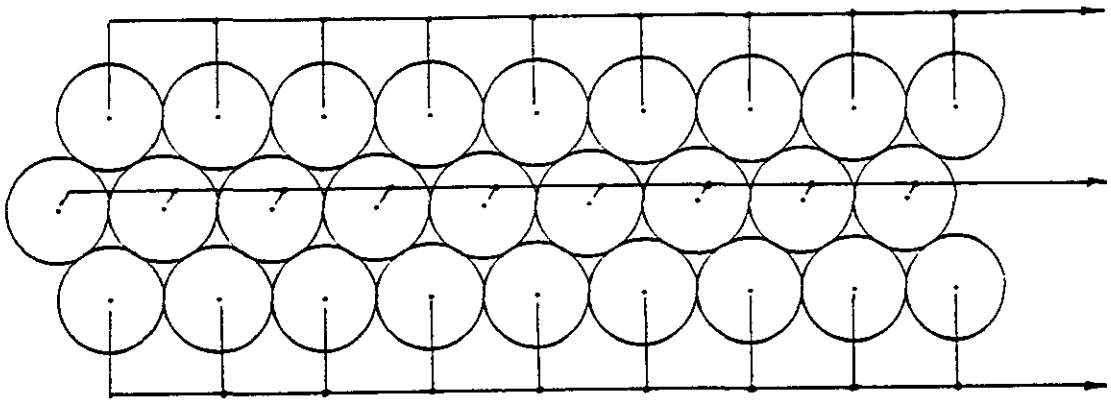

Fig.5.a.

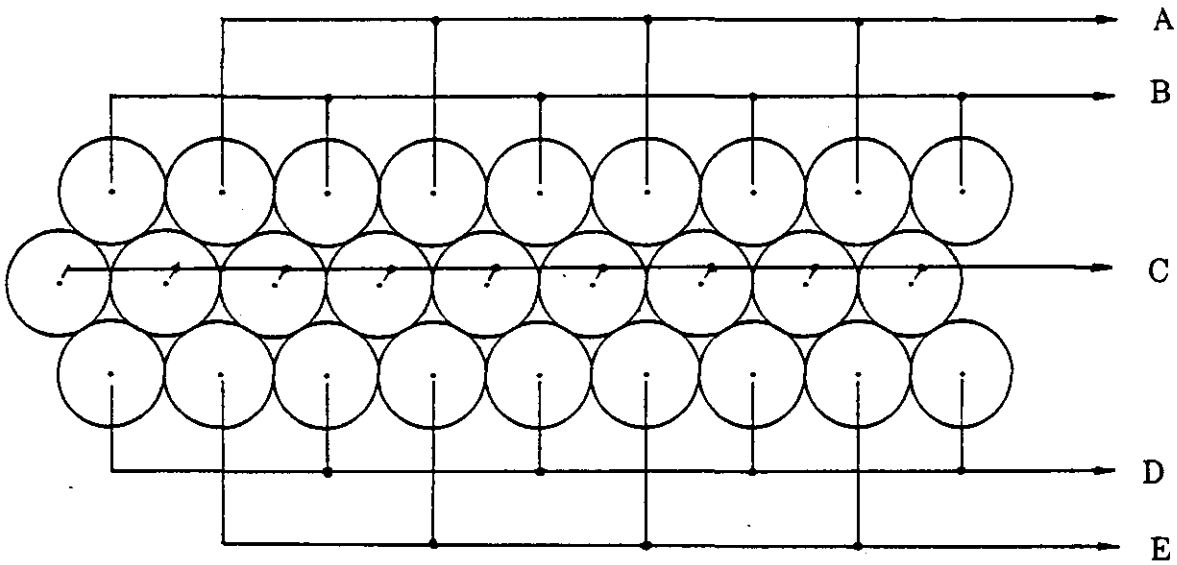

Fig.5.b.

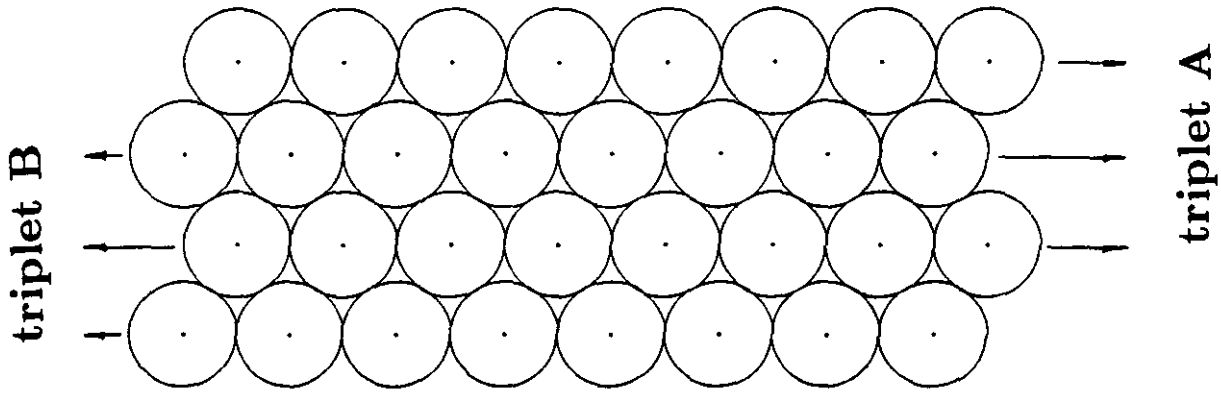

Fig.5.c.

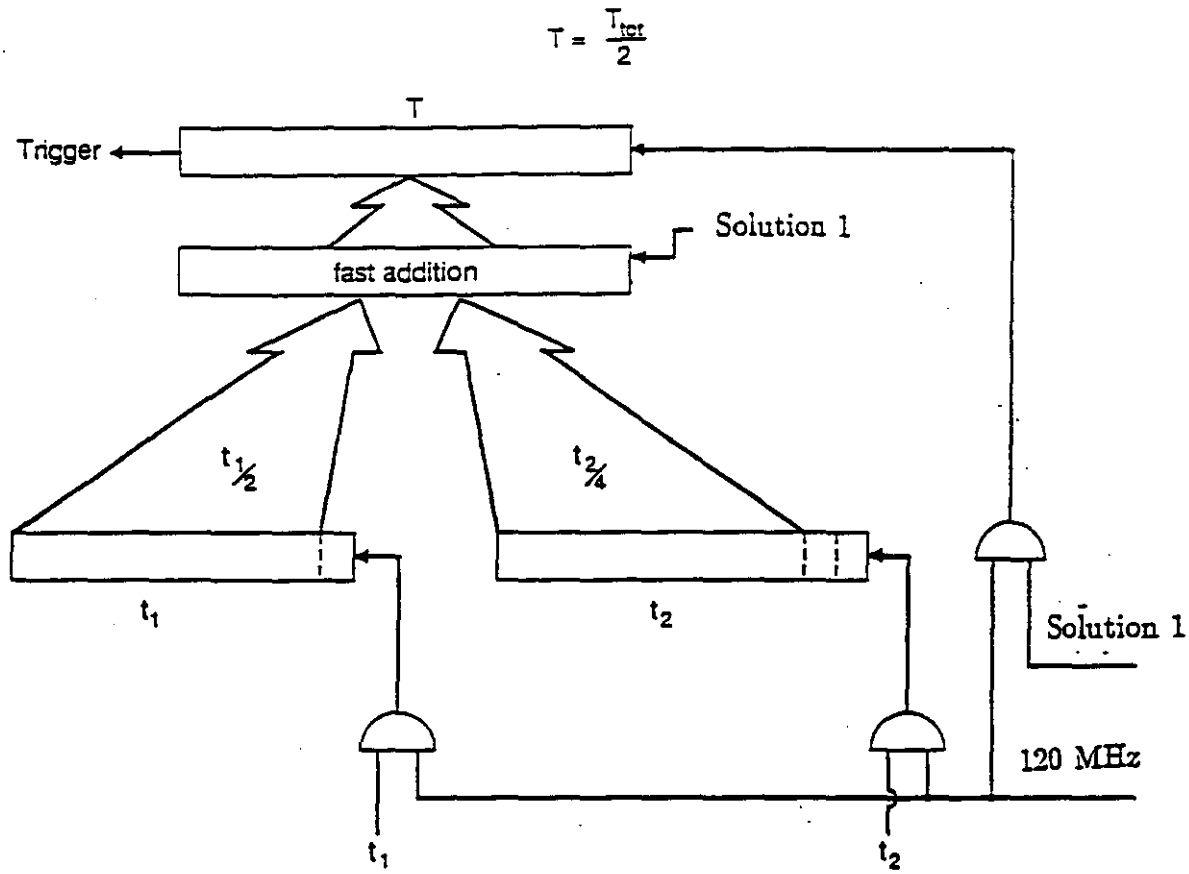
T = Tcer / 2
T
Trigger
Solution 1
fast addition
t1/2
t2/4
t1
t2
Solution 1
120 MHz
t1
t2

Fig.6.

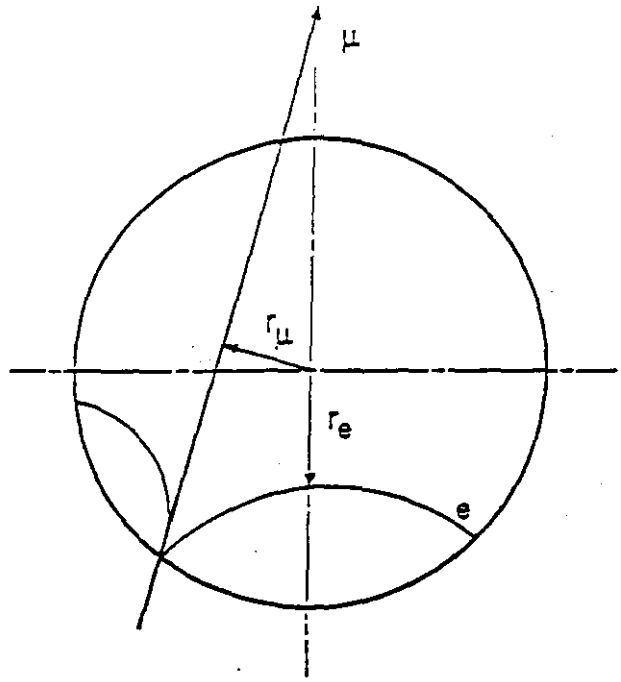

Fig.7.